

Nature of Sub-Band Gap Luminescent Eigenmodes in a ZnO Nanowire

S. Rühle,[†] L. K. van Vugt,[†] H.-Y. Li,[†] N. A. Keizer,[†] L. Kuipers,[‡] and D. Vanmaekelbergh^{*,†}

Condensed Matter and Interfaces, Institute for Nanomaterials Science, Utrecht University, P.O. Box 80 000, 3508 TA Utrecht, The Netherlands, and Center for Nanophotonics, FOM Institute for Atomic and Molecular Physics (AMOLF), Kruislaan 407, 1098 SJ Amsterdam, The Netherlands

Received August 29, 2007; Revised Manuscript Received October 29, 2007

ABSTRACT

The emission spectrum of individual high-quality ZnO nanowires consists of a series of Fabry–Pérot-like eigenmodes that extend far below the band gap of ZnO. Spatially resolved luminescence spectroscopy shows that light is emitted predominantly at both wire ends, with identical spectra reflecting standing wave polariton eigenmodes. The intensity of the modes increases supralinearly with the excitation intensity, indicating that the mode population is governed by scattering among polaritons. Due to strong light–matter interaction, light emission from a ZnO nanowire is not dictated by the electronic band diagram of ZnO but depends also on the wire geometry and the excitation intensity. Delocalized polaritons provide a natural explanation for the pronounced subwavelength guiding in ZnO wires that has been reported previously.

The research field of semiconductor nanowires has been expanding rapidly in the last years due to the promise of applications in logic and memory devices,^{1,2} sensors,^{3,4} miniaturized optoelectrical devices such as LEDs^{5,6} and lasers,^{7–9} and circuits for optical information transfer.¹⁰ Nanowires of II–VI semiconductor compounds, such as CdS and ZnO, and the III–V compound GaN are currently attracting a strong interest due to their intriguing optical properties. For instance, single wires show lasing under optical excitation; strikingly, the lasing light has a wavelength that is larger than the diameter of the semiconductor wire.^{8,9,11,12} The technological relevance of these results is demonstrated by the first electrically driven laser device based on a CdS nanowire.⁷ Furthermore, efficient guiding of UV and visible light has been reported in nanowires that consist of ZnO, SnO₂, and CdS.^{13,14} Remarkably, the guided light has, in many cases, a vacuum wavelength larger than the wire diameter. This phenomenon has been called “active wave guiding” in the literature.¹⁴ Despite the potential of semiconductor nanowires for photonic applications, the physics that underlie the optical properties has not yet received great attention. For instance, the mechanism of luminescence and lasing in nanowires of II–VI semiconductors is unclear: are free electrons and holes involved or excitons, and to what extent is light–matter interaction in the wire playing a role? Furthermore, the nature of the

excitations that mediate the “active” light guiding in nanowires has not been studied in detail. Semiconductor nanowires form a relatively new field, and the level of physical understanding is considerably less than that of planar semiconductor cavities, where exciton–photon conversion and interaction has been studied in much detail.^{15–17} In the present work, we present new results on the light emission from a ZnO nanowire, which can only be understood if a strong light–matter interaction is taken into account.

ZnO crystals possess remarkable optoelectronic properties such as three exciton resonances (A, B, and C exciton) due to spin–orbit coupling in the crystal field with a large oscillator strength and an exciton binding energy up to 60 meV.¹⁸ As a consequence, it is expected that the light–matter interaction is very strong and that exciton–polariton quasiparticles are the fundamental excitations.¹⁹ For macroscopic crystals and thin films of ZnO, strong exciton–photon coupling has been observed from angle-dependent absorption, reflection, and luminescence spectroscopy at cryogenic temperatures.^{19–21} It has been predicted that due to photon confinement, the light–matter interaction should be enhanced in ZnO nanostructures.²² Recently, we have studied the excitation spectrum of ZnO nanowires. This work showed that in a nanowire geometry, excitonic light absorption is governed by strong exciton–photon coupling, even at room temperature.²³

Here, we present intriguing emission properties of single, individual ZnO nanowires at room temperature. We found that the luminescence spectrum extends in energy to far

* To whom correspondence should be addressed. E-mail: d.vanmaekelbergh@uu.nl.

[†] Utrecht University.

[‡] AMOLF.

below the band gap of ZnO. The nature of the luminescence has been studied by spatially resolved luminescence spectroscopy. We observe that most of the light is emitted via the wire ends. The spectra collected at both of the wire ends are identical and consist of a series of peaks. The spacing between the peaks scales with the inverse wire length, showing that the peaks reflect Fabry–Pérot eigenmodes delocalized over the wire. Further analysis shows that the modes are, in fact, polariton eigenmodes situated on the lower polariton branch. Light–matter interaction is strongly enhanced with respect to macroscopic ZnO. The intensity of each of the polariton eigenmodes exhibits a power law dependence on the excitation intensity, with a power ranging from 1.5 at the higher-energy side to nearly 2 at the low-energy side of the spectrum. We attribute this nonlinear behavior to the population dynamics of the eigenmodes being governed by polariton–polariton scattering. The fact that the energy and intensity of the light emission from a ZnO nanowire is not only determined by the electronic band diagram but also depends on the wire dimensions and, in a nonlinear way, on the excitation intensity is highly important for ZnO nanowire-based optoelectrical devices. Furthermore, we show that the polariton nature of the eigenmodes in ZnO nanowires revealed in the present study explains the previously reported subwavelength guiding.

ZnO wires were grown epitaxially on a sapphire substrate using a vapor–liquid–solid method at high temperature (960 °C), with gold droplets as a catalyst.²⁴ The wires were single-crystalline, the *c* axis being the long axis, and the sides were faceted; the length of the wires was between 2 and 8 μm , and the lateral dimensions were between 200 and 400 nm. After growth, the wires were transferred to a silica substrate for a microscopic study. The (spatially resolved) luminescence of a single wire was studied with an adapted luminescence microscope (Zeiss Axioplan 2). Single wires lying on the substrate were homogeneously excited with a pulsed Nd:YLF laser at a wavelength of 349 nm (10 ns pulse length, 1.6 kHz repetition rate, corresponding to a time-averaged cw power density of maximal 1200 W/cm²). Neutral density filters were used to change the excitation power density. The energy of the excitation (3.54 eV) was considerably above the exciton resonances (3.31–3.35 eV at room temperature). A spatially resolved far-field emission spectrum was acquired by scanning the wire with a piezoelectric translator stage (PI) under the microscope with a pinhole mounted in the image plane of the microscope. The luminescence was collected with an optical fiber mounted behind the pinhole and analyzed with a spectrophotometer (SpectraPro 300i, Acton Research) and a liquid-nitrogen-cooled CCD (Roper Scientific). The spatial resolution that we obtained was about 500 nm. The wire dimensions were determined by SEM. The luminescence spectra of tens of ZnO wires of different lengths have been studied.

Figure 1 summarizes the emission properties of a typical ZnO nanowire (4.9 μm in length and 200 nm in diameter as determined by SEM) at a given excitation intensity. Figure 1a shows luminescence spectra acquired at both ends and the central part of the wire. Luminescence is observed from

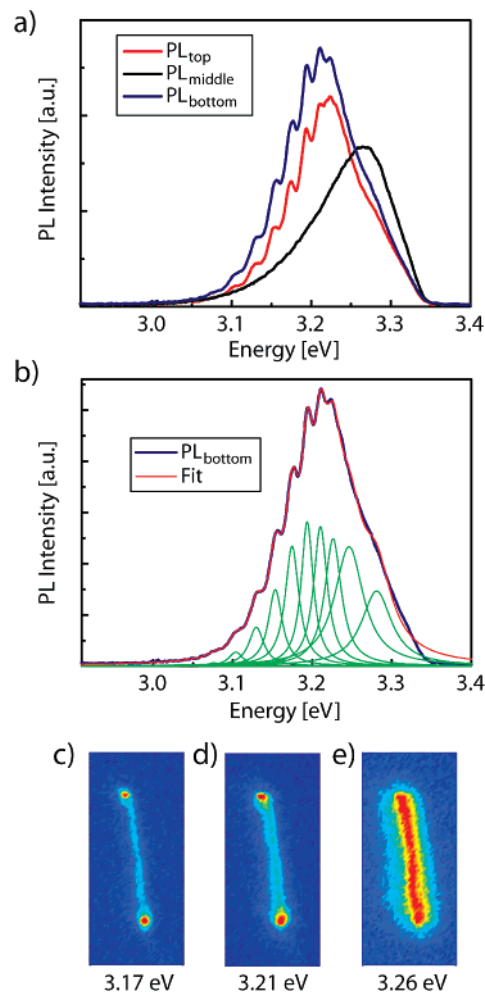


Figure 1. Spatially resolved emission spectra of a ZnO nanowire (4.9 μm long, 200 nm diameter) homogeneously excited above resonance with a 349 nm laser beam with an intensity of 2.3 W/cm². (a) Emission spectra obtained at both wire ends (red and blue) and in the central part of the wire (black). (b) Analysis of the emission spectrum at the bottom end as a sum of Fabry–Pérot peaks each with a Lorentzian line shape. (c–e) Map of the emission intensity along the wire at three different photon energies.

3.34 eV (close to the electronic band gap) extending to below 3 eV. This luminescence is not due to shallow defects. At cryogenic temperatures, luminescence from donor-bound exciton states in the energy region at around 3.36 eV has been reported. However, this luminescence quenches rapidly with increasing temperature due to the weak binding energy between the donor and the exciton.^{25,26} As a consequence, free excitons prevail at room temperature. The spectra detected at both wire ends are identical and consist of a series of peaks, in contrast to those taken over the central part of the wire. Figure 1b shows that these spectra can be fitted to a sum of Lorentzians, where each Lorentzian (except the two at the highest energy) represents an individual luminescence peak.

Figure 1c–e presents the spatially resolved emission patterns for photon energies of 3.17, 3.21, and 3.26 eV, respectively. Photons with 3.26 eV energy (close to the exciton resonance) are detected with a uniform intensity over the entire wire (Figure 1e). In contrast, below 3.22 eV (in

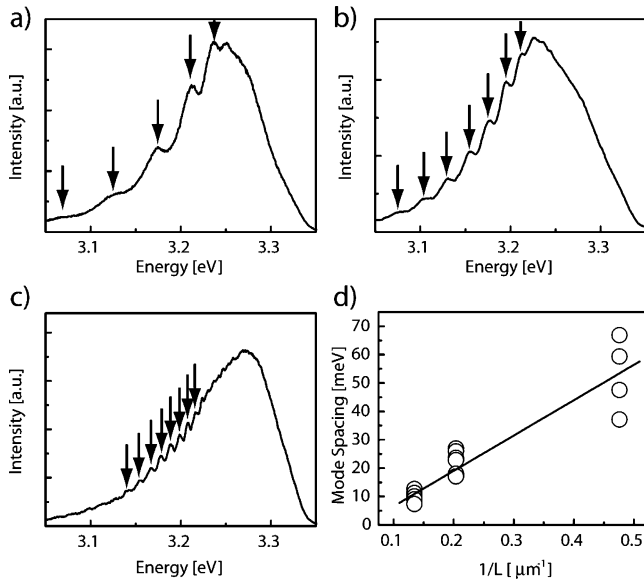


Figure 2. Photoluminescence spectra with pronounced Fabry–Pérot interferences of (a) 2.1, (b) 4.9, and (c) 7.5 μm long nanowires. (d) The mode spacings as a function of the inverse nanowire length L . For a given wire, the spacing decreases with increasing mode number. The solid line shows a least-square fit.

the region with pronounced peaks), light is predominantly emitted at the wire ends (Figure 1c,d). Since the emission spectra at both of the wire ends feature a series of identical peaks, it is very likely that they reflect standing-wave eigenmodes in the ZnO nanowire. Examination of the spectra of several wires shows that the spacing between the peaks in the emission spectrum becomes smaller with increasing wire length; see Figure 2. The spectrum of a 2.1 μm long wire shows that the average spacing is around 55 meV (Figure 2a), while it is 23 meV for a 4.9 μm long wire (Figure 2b) and 10 meV for a 7.5 μm long wire (Figure 2c). Note that the spacing decreases with increasing mode number (see below). The mode spacings are approximately linearly dependent on the inverse nanowire length (Figure 2d). Hence, we attribute the luminescence maxima detected at the wire ends to a series of standing-wave Fabry–Pérot modes with the wavevector parallel to the wire’s long axis ($k = k_{\parallel}$).

The luminescence spectra of single wires reflecting Fabry–Pérot-like eigenmodes were systematically studied under variation of the excitation intensity over a wide range; typical results are presented in Figure 3. Figure 3a presents the logarithm of the emission intensity versus the photon energy. The dashed lines represent the energy of the eigenmodes; it can be seen that above an excitation intensity of 6.9 W/cm^2 , they shift slightly toward higher energy with increasing excitation intensity. We have fitted each emission spectrum to a sum of Lorentzian peaks (similar as that in Figure 1b) and analyzed the integrated intensity of each mode as a function of the excitation power; see Figure 3b. The intensity of the individual modes i increases supralinearly with the excitation intensity, that is, $I_{\text{em}}(i) \sim I_{\text{ex}}^{\gamma(i)}$. The power law did not vary markedly for wires of different lengths below 5 μm , for which the modes can be spectrally resolved at all excitation intensities. The exponent $\gamma(i)$ is close to 1.6 for the modes at a higher energy and increases

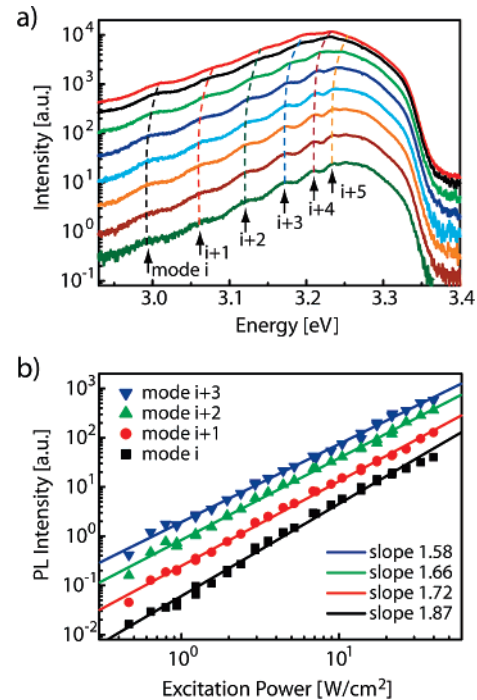


Figure 3. Dependence of the Fabry–Pérot peaks in the emission spectrum on the excitation intensity of a ZnO nanowire (2.1 μm long, 265 nm diameter). (a) Plots of the emission spectra (logarithmic scale) at different excitation intensities (green, 0.3 W/cm^2 ; brown, 0.9 W/cm^2 ; orange, 2.0 W/cm^2 ; blue, 3.6 W/cm^2 ; mauve, 6.9 W/cm^2 ; green, 13.8 W/cm^2 ; black, 26.7 W/cm^2 ; red, 39.8 W/cm^2). The dashed lines indicate the evolution of the position of the peak maxima with the excitation intensity. (b) Emission intensity of four peaks selected from the spectrum as a function of the excitation intensity; the emission spectrum increases supralinearly with the excitation intensity in all cases.

to nearly 2 for the modes at the low-energy side of the spectrum. In other words, the lower-energy modes in the spectrum become relatively more pronounced with increasing excitation intensity. In Figure 3a, it can be observed that the Fabry–Pérot peaks become somewhat broader at higher intensity. In general, the peak width depends on the length of the wire, the mode number, and the excitation intensity. If we convert a typical value of the FWHM for the 2.1 μm long nanowire (~ 40 meV) into a lifetime, values on the order of ~ 10 fs are found. Remark that this is orders of magnitude smaller than the decay time of an exciton in bulk ZnO.²⁷

From Figure 3a, it can be observed that at all excitation intensities, the energy spacings between neighboring modes become smaller with increasing energy approaching the exciton resonance. This shows that the modes do not correspond to classical Fabry–Pérot light modes in the ZnO resonator. For a fundamental understanding of the luminescence spectrum, it is required to take the coupling between excitons and confined photons into account. Figure 4a (left-hand side) shows a plot of the peaks (data taken from the wire of Figure 3) in the energy–wavevector diagram, $E-k_{\parallel}$ diagram. The blue curve shows the dispersion of photons confined in the ZnO nanowire (2.1 μm long, 265 nm in diameter); the cutoff at around 2 eV is due to lateral confinement of the photons in the wire, that is, a half-wavelength equal to the wire diameter. The next lateral mode

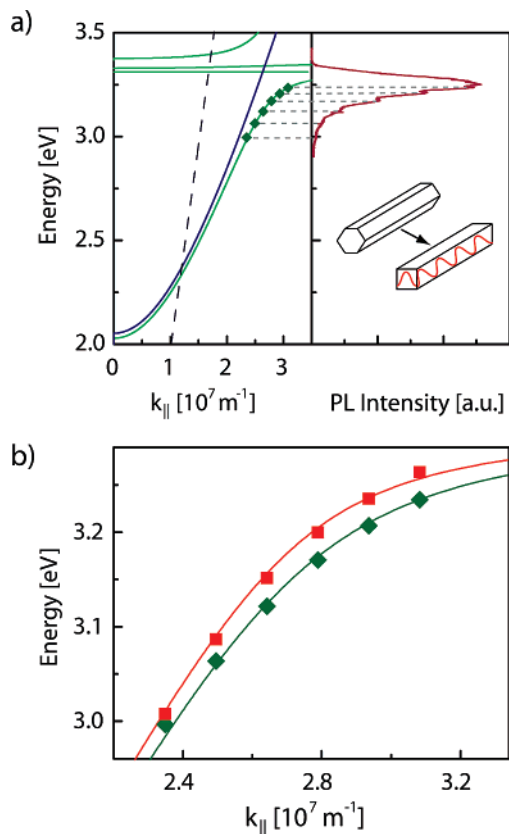


Figure 4. Fit of the Fabry–Pérot peaks to the polariton equation (error bars due to the fit of Lorentzian peaks in the spectra, see Figure 1b, are smaller than the size of the symbols). (a) Left: Plots of the photon dispersion in vacuum (dashed line), the dispersion curve of photons confined in the nanowire (blue) and the polariton dispersion curve (green) for the wire studied in Figure 2. The Fabry–Pérot peaks (green diamonds) deviate from the photon line but can be fitted with the polariton equation, taking into account an enhanced oscillator strength. (b) Dispersion curve for the modes observed at excitation intensities of 39.8 (squares) and 0.5 W/cm² (diamonds); the modes can be fit with the polariton dispersion curve. Low intensity, 5.5 times enhanced oscillator strength; high-intensity, 3.8 times enhanced oscillator strength.

has a cutoff at around 3.1 eV and can be safely disregarded. It can be seen that the Fabry–Pérot modes of the luminescence spectrum cannot be fitted with the confined photon dispersion. The deviation between the photon line and experimental $E-k_{||}$ points becomes stronger with increasing emission energy approaching the exciton resonance. This indicates that the emission spectrum is determined by strong exciton–photon coupling in the ZnO nanowire. We have therefore used the polariton equation²⁸ to analyze our results. Figure 4a shows the polariton branches calculated for the ZnO nanowire under study (see also Figure 3). It can be seen that the Fabry–Pérot emission modes are situated on the lower polariton branch. We remark that the emission from the upper polariton branch and the band edges (above 3.37 eV) is very weak. A good fit of the modes with the polariton equation is obtained only if the oscillator strength is 5.5-fold enhanced with respect to that of a macroscopic ZnO crystal. Similar results have been obtained with other wires with lengths between 1 and 6 μm and diameter between 200 and 400 nm. At low excitation intensity, the mode energy

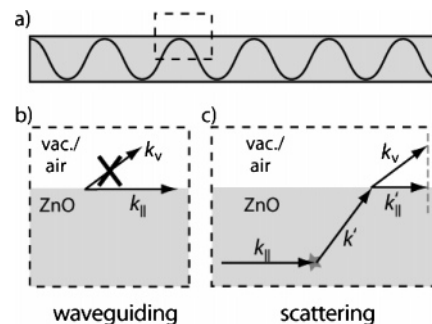


Figure 5. Polariton guiding in a ZnO nanowire. (a) Schematic of a standing-wave polariton in a wire. (b) Magnification of the ZnO/air interface; modes with $k_{||}$ larger than the wavevector k_v in free space (at the same energy) cannot escape through the sides of the wire and are hence guided. (c) Exciton polariton modes that are scattered may escape through the sides of the wire (k' is the wavevector of the scattered mode, with a parallel projection $k'_{||}$).

remains constant, but at higher intensities, there is a slight blue shift of the modes (see Figure 3a). This is further demonstrated in Figure 4b, which presents a plot of the modes in the $E-k_{||}$ diagram for two excitation intensities; for the lower excitation intensity (diamonds), a fit to the polariton dispersion curve shows that the oscillator strength is 5.5-fold enhanced, while for the larger excitation intensity (squares), the enhancement is 3.8 compared to a macroscopic ZnO crystal. These results show that exciton–photon coupling in ZnO nanowires at room temperature is very strong and becomes only weakened at higher excitation intensities.

The luminescent polariton modes located on the lower branch have a considerably larger wavevector $k_{||}$ than that of vacuum light modes (dashed line in Figure 4a). Hence, due to conservation of energy E and the wavevector $k_{||}$, escape of these polaritons is forbidden along the length of the wire; see Figure 5b. The wavevector parallel to the end facet is zero or very small; polaritons at the end facets are hence partially reflected and partially transmitted into the vacuum. This explains why the polariton modes are guided, that is, predominantly detected at both wire ends (see Figure 1). The emission detected above the central part of the wire must hence be considered as a cavity loss, very probably due to scattering between polaritons or between polaritons and phonons (see Figure 5c). Light of energy at around 3.26 eV is emitted uniformly over the wire, meaning that the modes at this energy are not guided. We attribute this to the strong exciton character of the highest energy modes together with the high mode density in this energy region; these two factors favor scattering of polaritons with themselves and with acoustic phonons. The work presented here strongly indicates that the striking subwavelength guiding in ZnO nanowires¹³ is, in fact, mediated by delocalized exciton polaritons of the lower branch. The large wavevector of these modes (at around $25 \times 10^6/\text{m}$) together with the considerable delocalization (over a length of at least 10 μm) ensures efficient guiding, even through bent parts of the wire, as has been demonstrated.¹³

The emission that we detect is mainly due to polaritons that leave the wire at the ends. It is reasonable to assume that the escape probability of a given polariton mode at the

wire ends is independent of the polariton density. This means that the emission intensity at a given $E-k_{\parallel}$ point should be proportional to the polariton occupation at this point. However, we observe that the intensity of each mode in the luminescence spectrum increases supralinearly with the intensity of the nonresonant excitation (Figure 3). This strongly indicates that the population dynamics of the guided $E-k_{\parallel}$ mode itself is a nonlinear process. Most reasonably, the population dynamics is governed by nonelastic scattering among exciton–polaritons. We remark that also phonon release/uptake by exciton polaritons could play a role. The competition between polariton–polariton and polariton–phonon scattering can explain the gradually varying exponent $\gamma(i)$ between 1.6 at high mode numbers and almost 2 at the lower mode numbers.

In summary, we have shown that light emission by a ZnO nanowire is governed by a strong light–matter interaction. The emission spectrum and the emitted intensity cannot be explained on the basis of the electronic band diagram and exciton oscillator strength; the dimensions of the wire and the excitation density are equally important factors. The observation that light emission extends to far below the band gap and increases supralinearly with excitation density is important for ZnO nanowire-based light sources. The polariton emission increasing supralinearly with the excitation power can effectively suppress nonradiative exciton decay, which means that, in principle, the photoluminescence quantum yield can approach unity even if the ZnO lattice and the nanowire surface contain natural electronic defects. Our results also provided a natural explanation for the striking guiding in ZnO nanowires that has been reported previously.

Acknowledgment. This work is supported by NanoNed, a national nanotechnology program coordinated by the Dutch Ministry of Economic Affairs. Furthermore, this work is part of the research program of the “Stichting voor Fundamenteel Onderzoek der Materie (FOM)” and a CW Topgrant (700.53.308) that are financially supported by the Nederlandse Organisatie voor Wetenschappelijk Onderzoek (NWO).

References

- (1) Huang, Y.; Duan, X. F.; Cui, Y.; Lauhon, L. J.; Kim, K. H.; Lieber, C. M. Logic gates and computation from assembled nanowire building blocks. *Science* **2001**, *294*, 1313.
- (2) Jung, Y.; Lee, S.-H.; Ko, D.-K.; Agarwal, R. Synthesis and characterization of Ge₂Sb₂Te₅ nanowires with memory switching effect. *J. Am. Chem. Soc.* **2006**, *128*, 14026.
- (3) Patolsky, F.; Zheng, G.; Lieber, C. M. Nanowire-based biosensors. *Anal. Chem.*, **2006**, *78*, 4260.
- (4) Sirbully, D. J.; Tao, A.; Law, M.; Fan, R.; Yang, P. D. Multifunctional nanowire evanescent wave optical sensors. *Adv. Mater.* **2007**, *61*, 66.
- (5) Huang, Y.; Duan, X. F.; Lieber, C. M. Nanowires for integrated multicolor nanophotonics. *Small* **2005**, *1*, 142.
- (6) Minot, E. D.; Kelkensberg, F.; van Kouwen, M.; van Dam, J. A.; Kouwenhoven, L. P.; Zwiller, V.; Borgstrom, M. T.; Wunnicke, O.; Verheijen, M. A.; Bakkers, E. P. A. M. Single quantum dot nanowire LEDs. *Nano Lett.* **2007**, *7*, 367.
- (7) Duan, X. F.; Huang, Y.; Agarwal, R.; Lieber, C. M. Single-nanowire electrically driven lasers. *Nature* **2003**, *421*, 241.
- (8) Huang, M. H.; Mao, S.; Freik, H.; Yan, H. Q.; Wu, Y. Y.; Kind, H.; Weber, E.; Russo, R.; Yang, P. D. Room-temperature ultraviolet nanowire nanolasers. *Science* **2001**, *292*, 1897.

- (9) van Vugt, L. K.; Rühle, S.; Vanmaekelbergh, D. Phase-correlated nondirectional laser emission from the end facets of a ZnO nanowire. *Nano Lett.* **2006**, *6*, 2707.
- (10) Sirbully, D. J.; Law, M.; Pauzauskie, P.; Yan, H. Q.; Maslov, A. V.; Knutsen, K.; Ning, C. Z.; Saykally, R. J.; Yang, P. D. Optical routing with nanoribbons and nanowire assemblies. *Proc. Nat. Acad. Sci.* **2005**, *102*, 7800.
- (11) Gradecak, S.; Qian, F.; Li, Y.; Park, H. G.; Lieber, C. M. GaN nanowire lasers with low lasing thresholds. *Appl. Phys. Lett.* **2005**, *87*, 173111.
- (12) Agarwal, R.; Barrelet, C. J.; Lieber, C. M. Lasing in single cadmium sulfide nanowire optical cavities. *Nano Lett.* **2005**, *5*, 917.
- (13) Law, M.; Sirbully, D. J.; Johnson, J. C.; Goldberger, J.; Saykally, R. J.; Yang, P. D. Nanoribbon waveguides for subwavelength photonics integration. *Science* **2004**, *305*, 1269.
- (14) Barrelet, C. J.; Greytak, A. B.; Lieber, C. M. Nanowire photonic circuit elements. *Nano Lett.* **2004**, *4*, 1981.
- (15) Weisbuch, C.; Nishioka, M.; Ishikawa, A.; Arakawa, Y. Observation of the coupled exciton–photon mode splitting in a semiconductor quantum microcavity. *Phys. Rev. Lett.* **1992**, *69*, 3314.
- (16) Khitrova, G.; Gibbs, H. M.; Jahnke, F.; Kira, M.; Koch, S. W. Nonlinear optics of normal-mode-coupling semiconductor microcavities. *Rev. Mod. Phys.* **1999**, *71*, 1591.
- (17) Kasprzak, J.; Richard, M.; Kundermann, S.; Baas, A.; Jeambrun, P.; Keeling, J. M. J.; Marchetti, F. M.; Szymanska, M. H.; Andre, R.; Staehli, J. L.; Savona, V.; Littlewood, P. B.; Deveaud, B.; Dang, L. S. Bose–Einstein condensation of exciton polaritons. *Nature* **2006**, *443*, 409.
- (18) Thomas, D. G. The exciton spectrum of zinc oxide. *J. Phys. Chem. Solids* **1960**, *15*, 86.
- (19) Hopfield, J. J.; Thomas, D. G. Polariton absorption lines. *Phys. Rev. Lett.* **1965**, *15*, 22.
- (20) Lagois, J. Depth dependent eigen energies and damping of excitonic polaritons near a semiconductor surface. *Phys. Rev. B: Condens. Matter* **1981**, *23*, 5511.
- (21) Toropov, A. A.; Nekrutkina, O. V.; Shubina, T. V.; Gruber, T.; Kirchner, C.; Waag, A.; Karlsson, K. F.; Holtz, P. O.; Monemar, B. Temperature-dependent exciton polariton photoluminescence in ZnO films. *Phys. Rev. B: Condens. Matter* **2004**, *69*, 165205.
- (22) Zamfirescu, M.; Kovokin, A.; Gil, B.; Malpuech, G.; Kaliteevski, M. ZnO as a material mostly adapted for the realization of room-temperature polariton lasers. *Phys. Rev. B: Condens. Matter* **2002**, *65*, 161205.
- (23) van Vugt, L. K.; Rühle, S.; Ravindran, P.; Gerritsen, H. C.; Kuipers, L.; Vanmaekelbergh, D. Exciton-polaritons confined in a ZnO nanowire cavity. *Phys. Rev. Lett.* **2006**, *97*, 147401.
- (24) Prasanth, R.; van Vugt, L. K.; Vanmaekelbergh, D. A. M.; Gerritsen, H. C. Resonance enhancement of optical second harmonic generation in a ZnO nanowire. *Appl. Phys. Lett.* **2006**, *88*, 181501.
- (25) Hsu, H.-C.; Hsieh, W.-F. Excitonic polaron and phonon assisted photoluminescence of ZnO nanowires. *Solid State Commun.* **2004**, *131*, 371.
- (26) Zhang, Y.; Chen, D.-J.; Lee, C.-T. Free exciton emission and dephasing in individual ZnO nanowires. *Appl. Phys. Lett.* **2007**, *91*, 161911.
- (27) Wilkinson, J.; Ucer, K. B.; Williams, R. T. The oscillator strength of extended exciton states and possibility for very fast scintillators. *Nucl. Instrum. Methods Phys. Res., Sect. A* **2005**, *537*, 66.
- (28) We calculated the exciton polariton dispersion curve for a ZnO nanowire using

$$\epsilon(\omega, k) = \epsilon_{\infty} \left(1 + \sum_{j=A,B,C} \Omega_j \frac{f_j}{\omega_{j,T}^2 - \omega^2} \right) = \frac{c^2(2k_{\perp}^2 + k_{\parallel}^2)}{\omega^2}$$

with the background dielectric constant ϵ_{∞} , the speed of light in vacuum c , the oscillator strength f_j , which can be expressed by the transverse ($\omega_{j,T}$) and longitudinal ($\omega_{j,L}$) resonance frequencies ($f_j = \omega_{j,L}^2 - \omega_{j,T}^2$), a prefactor Ω_j as defined in ref 20, and a factor Γ , which describes the enhancement of the oscillator strength. The resonant frequencies (for A, B, and C excitons) were taken as for a macroscopic ZnO crystal²⁰ with the resonance frequencies shifted to room temperature. We approximated the hexagonal ZnO nanowire by a nanowire cavity with a rectangular cross section with $k_{\perp} = \pi/d$ as the wavevector perpendicular to the nanowire long axis (d is the nanowire diameter).

NL0721867